Measurement of Tokamak Plasma with the External Helical Field Using a High-Speed Camera in TOKASTAR-2*)

Tatsuya SAKITO, Hideki ARIMOTO, Takaaki FUJITA, Atsushi OKAMOTO, Yusuke SHIMOOKA, Hiromasa ITOU, Ryoichi SUGIOKA, Kenji MURAOKA, Kouhei YASUDA and Ryoma YOKOYAMA

Department of Energy Engineering and Science, Nagoya University, Furo-cho, Chikusa-ku, Nagoya 464-8603, Japan

(Received 30 November 2015 / Accepted 23 March 2016)

The high-speed camera was used to evaluate the position of the plasma in TOKASTAR-2. A plane mirror was installed in the vacuum vessel to expand the field of view and get the image in the whole region between inner and outer walls. The images were taken at 86400 FPS with 256 × 128 pixels (20 μm / pixel) per frame in the tokamak discharge with and without the external helical field. Under the condition of the weak vertical field, the plasma position control was improved by the external helical field. The outward plasma displacement was suppressed and the plasma was located stably in contact with the inner legs of the TF coils.

Keywords: high-speed camera, emission intensity, tokamak discharge, helical field application, TOKASTAR, tokamak-stellarator hybrid confinement

DOI: 10.1585/pfr.11.2402074

1. Introduction

The experiments of tokamak-stellarator hybrid devices indicated the effects of helical field on the stability of the plasma positon [1, 2] and on suppression of current disruptions which would exert the high heat flux and electromagnetic force to in-vessel components in tokamak devices [3, 4]. TOKASTAR-2 device was designed and constructed to study tokamak-stellarator hybrid confinement system with a low aspect ratio (A < 3) called TOKASTAR [5]. This device is able to generate tokamak and helical field configurations independently by using different types of coils. The main purpose of TOKASTAR-2 experiment is to study (i) the effect of helical field on tokamak plasma including stabilization of the plasma positon and suppression of disruption and (ii) equilibrium and stability of tokamak-helical hybrid configurations, both in the low aspect ratio (A < 3) region.

To improve tokamak plasma equilibrium control, we adjusted the vertical magnetic field [6, 7]. As a result, the peak value and duration of the plasma current of the tokamak discharge were increased. In this study, the effect of helical field application on tokamak plasma is evaluated. The plasma position are evaluated by the emission intensity distribution of the high-speed camera images taken in the tangential direction. We have installed a plane mirror in the vacuum vessel to expand the field of view, which was limited to the inner side previously [7].

2. Experimental Setup and Condition

2.1 TOKASTAR-2 device

The TOKASTAR-2 coil system has six kinds of coils; eight Toroidal Field (TF) coils, three-block Ohmic Heating (OH) coils, a pair of Pulsed Vertical Field (PVF) coils, a pair of static Vertical Field (VF) coils, two outboard Helical Field (HF) coils, and four Additional Helical Field (AHF) coils. The coil system of TOKASTAR-2 device is shown in Fig. 1. Capacitors are used in circuits for TF coils, OH coils and PVF coils, while DC power sources are used for VF coils, HF coils and AHF coils. VF coils are installed outside the vacuum vessel and the other coils are in it. The plasma is limited by the surfaces of legs of TF coils, to 65 mm ≤ R ≤ 180 mm in the radial direction. The inner legs of TF coils are covered by stainless steel plates as the limiters. The upper and lower PVF coils are connected in parallel in the experiment. In this paper, the sum of currents in these two coils, namely the current in

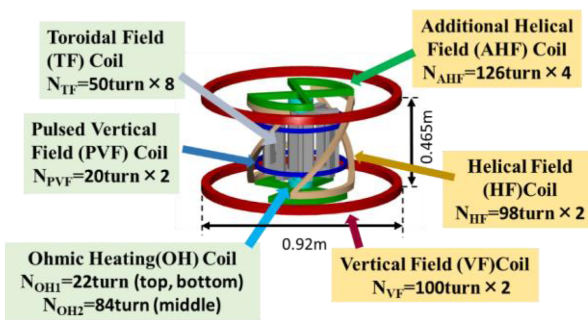

Fig. 1 Coil system of TOKASTAR-2 device.

author's e-mail: fujita@ees.nagoya-u.ac.jp

*) This article is based on the presentation at the 25th International Toki Conference (ITC25).

the PVF coil circuit, is used as the ‘PVF coil current’.

The magnetic field strength is $B_t R \sim 0.01$ Tm. In typical configuration, the plasma has a major radius of $R_p \sim 12$ cm and a minor radius of a ~ 5 cm. The electron cyclotron resonance (ECR) heating (2.45 GHz) is used for the pre-ionization and the injection power is ~ 1.4 kW. In this study, nitrogen gas was used as working gas.

In TOKASTAR-2, one-turn loops are installed at the four inner corners of the TF coils ($R = 0.06$ m, $Z = \pm 0.13$ m and $R = 0.18$ m, $Z = \pm 0.10$ m) to measure applied loop voltage in the toroidal direction. The voltage of inside one-turn loops is mainly affected by the magnetic flux change due to the OH coil current and the voltage of the outside loops is affected by the magnetic flux change due to OH coil and PVF coil current.

2.2 High-speed camera view

The left side drawing of Fig. 2 shows the top view of TOKASTAR-2 device and the camera sightlines. In the previous measurements, the field of view was limited to $R \leqq 115$ mm due to the window flange and the outer leg of a TF coil ($\phi = -67.5°$) [7]. In order to expand the field of view, we installed a surface plane mirror and a structure for supporting the mirror and adjusting its angle. The mirror can be accessed from the horizontal port. The size of the mirror is 97 mm width × 130 mm height × 5 mm thickness. The camera lens was also changed from a F-mount lens (f = 50 mm) to a wide-angle lens (C-mount lens f = 16 mm). The photograph of the view in the tangential direction is shown in the right side drawing of Fig. 2. It shows that the image in the mirror includes the whole region between inner and outer walls.

In this paper, we use images taken by a high-speed camera (FASTCAM SA4); a frame of 256 × 128 pixels (20 µm / pixel) at 86400 frames per second (FPS) was used. The area (number of pixels) of the camera image is reduced with increase in the frame rate. The frame rate 86400 FPS was the fastest speed keeping the area size covering the range of $65 \leq R \leq 180$ mm. The image was roughly equivalent to the area surrounded with the light green dotted line in Fig. 2 (Right). The aperture diaphragm value was F8. The point of focus was adjusted on the cross-section of

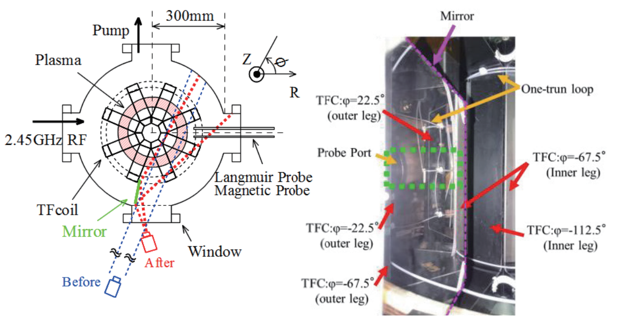

Fig. 2 (Left) Top view of high-speed camera sightlines. (Right) Photograph of the view in the tangential direction.

$\varphi = -22.5°$. Light emission from the plasma in front of and behind the focused cross-section was also taken on the images by the line integral effect because the plasma was in the shape of a circular torus. The horizontal angle of view was $\sim 18°$ and the vertical angle of view was $\sim 9°$. The camera image acquisition was initiated by an external timing trigger synchronized with plasma operation sequence. The image data are transferred to a PC for storage and analysis.

3. Results and Discussion

To study the effect of the helical field application, the external helical field was applied to the tokamak plasma. The TF coils, the OH coils and the PVF coils are used for tokamak operation. The charging voltage of the capacitor for PVF coil circuit (V_{PVF}) was scanned from 0.35 kV to 0.50 kV, while those for TF coil and OH coil circuits were fixed constant ($V_{TF} = 1.0$ kV, $V_{OH} = 2.0$ kV). The VF coils, the HF coils and the AHF coils are used for the helical field generation. The coil current values were $I_{VF} = 0.15$ kAT, $I_{HF} = 2.55$ kAT, $I_{AHF} = 2.875$ kAT (DC power sources). These were driven constant during tokamak discharge. These values were determined to make closed magnetic surfaces using a magnetic field tracing code HSD [8, 9]. The ratios of I_{HF} and I_{AHF} to I_P are $I_{HF} / I_P \sim 1.3$ and $I_{AHF} / I_P \sim 1.4$ for $I_P \sim 2$ kA.

Figure 3 shows the peak values and durations of the

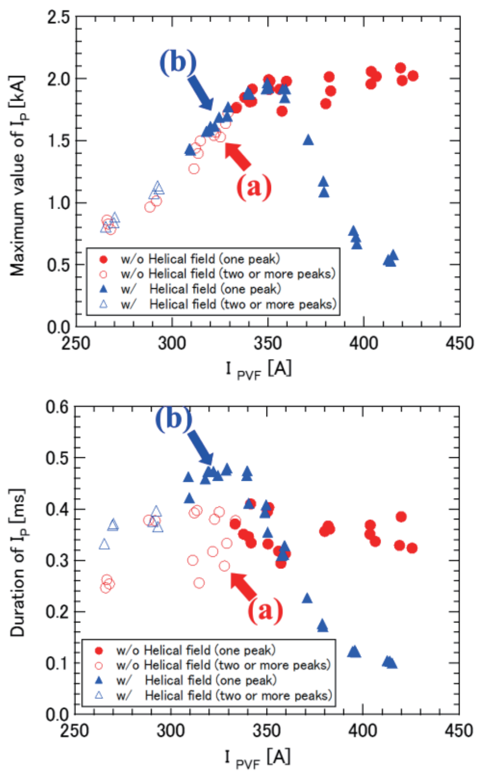

Fig. 3 (Top) The peak value of plasma current and (Bottom) the duration of plasma current as a function of the peak PVF coil current (I_{PVF}).

plasma current plotted as a function of the peak PVF coil current (I_{PVF}) in the tokamak discharge. "Duration of plasma current" was defined as the duration in which the value of plasma current was larger than 5% of the maximum value of plasma current in the discharge ($I_P \geqq 0.05\, I_{P\_max}$). The red circles denote the case without external helical field while the blue triangles denote the case with external helical field. Figure 4 shows time evolution of the PVF and OH coil currents (I_{PVF}, I_{OH}), the loop voltages and the plasma current for with and without the external helical field under the condition of V_{PVF} = 0.40 kV corresponding to I_{PVF} ~322 A. As shown in Fig. 4, temporal decreases were observed in the plasma current waveform (red curve). The legend "two or more peaks" in Fig. 3 denotes the discharges in which this phenomenon happened namely increases and decreases in the plasma current took place repeatedly. In Fig. 3, it was found that under the condition of weak vertical field (I_{PVF} < 350 A), the durations of the plasma current of tokamak discharge were extended by the external helical field. The plasma current waveform was also improved to a parabolic shaped waveform as shown by the blue curve in Fig. 4. The plasma current wave forms in the cases with the external helical field had one peak in the lower I_{PVF} discharges (310 A < I_{PVF} < 330 A), while those without helical coils had two or more peaks as shown in Fig. 3. Furthermore, the reproducibility of the tokamak discharge was improved by the external helical field.

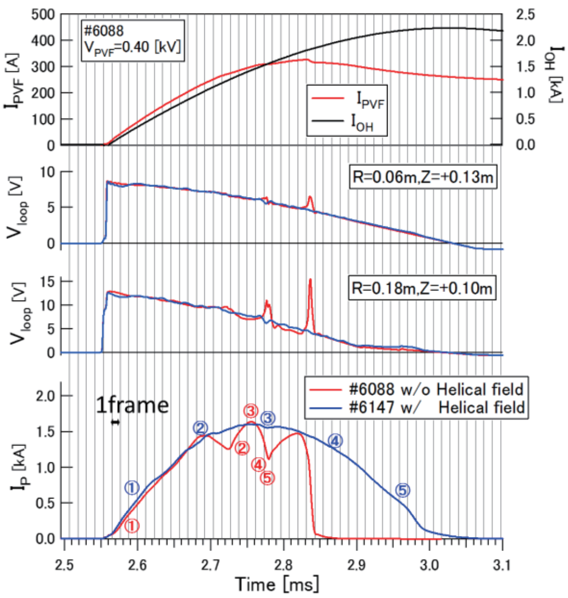

Fig. 4 Comparison of tokamak discharges with and without external helical field. From the top, the PVF coil and OH coil current, loop voltages at R = 0.06 m, Z = + 0.13 m and R = 0.18 m, Z = + 0.10 m and the plasma current waveform are shown. The red and blue curves denote the case without and with the external helical field, respectively.

Figure 5 shows a part of the images in tokamak discharge with and without the external helical field. The images are horizontally inverted because they were reflected by the mirror. Figure 6 shows the radial profile of the emission intensity averaged in the vertical direction at the time of 2.762 ms. To reduce the influence of the light reflected from the coil structures, it was processed that the emission intensity of the 128 pixels in the vertical direction was averaged. Figure 7 shows time evolution of the average emission intensity in the radial direction.

First, we discuss the tokamak discharge without external helical field. As shown in Fig. 5 (a), the position of the plasma initiation in the image at 2.588 ms (1st frame) was on the equatorial plane in contact with the inner legs of the TF coils. The plasma moved outward in the radial direction at 2.750 ms (3rd frame). At 2.773 ms (5th frame), the plasma disappeared and was generated on the inner legs of TF coils. In addition, the large spikes were observed in the outer loop voltage (R = 0.18 m, Z = + 0.10 m), accompanied by rapid decrease in the plasma current. It is considered that these spikes were caused by the plasma sudden disappearance and the instantaneous flux changes at the one-turn loops. This suggests that the plasma moved outward and was pressed in contact with the outer legs of TF coils at 2.762 ms (4th frame). As shown in Fig. 7 (a), sim-

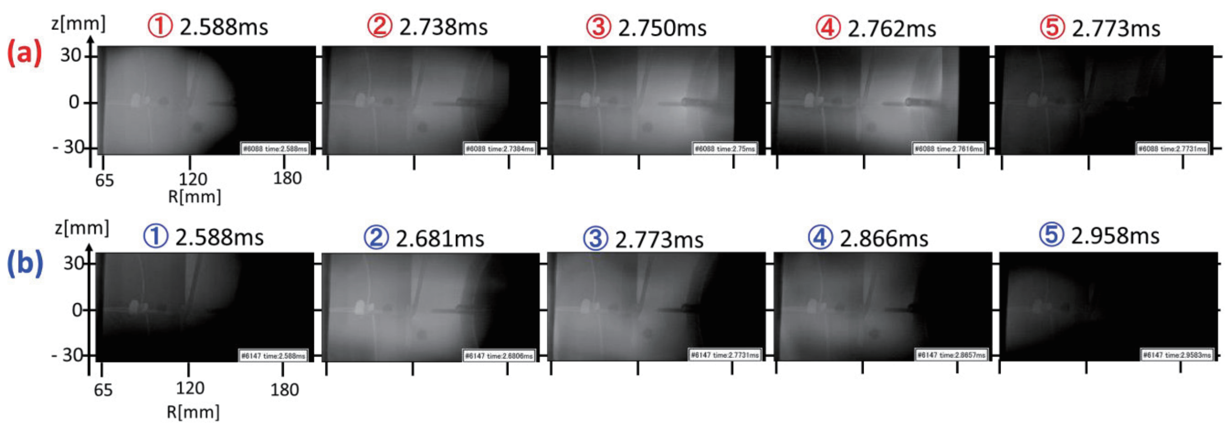

Fig. 5 Time evolution of images in tokamak discharge (a) without the external helical field and (b) with the external helical field.

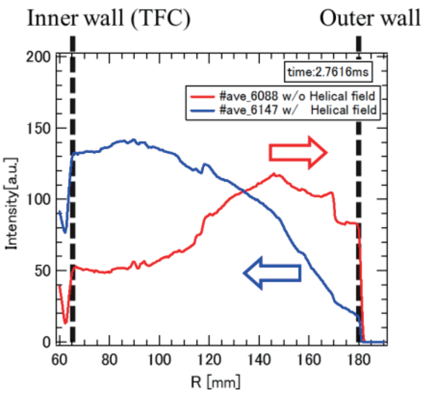

Fig. 6 Comparison of the radial profile of the average emission intensity averaged in the radial vertical direction at the time of 2.762 ms.

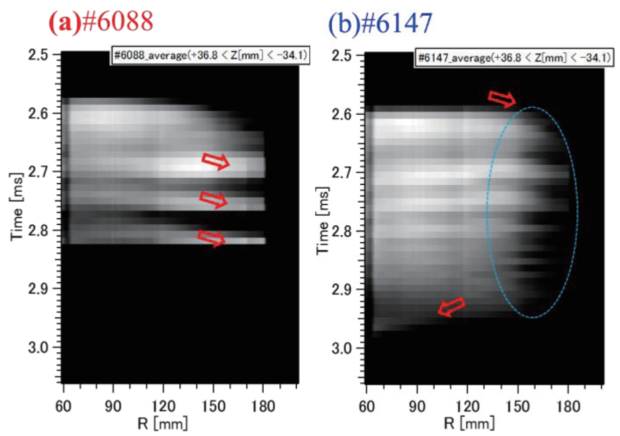

Fig. 7 Time evolution of the radial distribution of the emission intensity averaged in the vertical direction. (a) Discharge #6088 without the external helical field. (b) Discharge #6147 with the external helical field.

ilar phenomenon happened after ~ 2.82 ms and the plasma current decreased sharply.

On the other hand, in the tokamak discharge with external helical field the plasma current waveform was improved from the "two or more peaks" waveform to the parabolic shaped waveform. As a result, the durations of the plasma current of tokamak discharge were increased. It was observed that the plasma initiation location was above the equatorial plane (see the image at 2.588 ms (1st frame) in Fig. 5 (b)). As shown in Fig. 7 (b), immediately after the plasma initiation, the plasma was located at a larger major radius compared to tokamak discharge without external helical field. This suggests that when the plasma was located in the radial direction inward, the external helical field works as the opposite vertical field and forces the plasma to move outward. However, during the plasma current ramp up phase the outward plasma displacement was suppressed in tokamak discharge with the external helical field. This suggests that the external helical field works as the effective vertical field to push the plasma inward in the radial direction. In addition, the plasma was located stably and disappeared gradually during the decreasing phase of the plasma current in contact with the inner legs of the TF coils. Accordingly that external helical field contributed to the horizontal position stability of the radial direction in the tokamak discharge under the condition of $I_{PVF} < 350$ A.

4. Conclusions

The plasma position was evaluated by the emission intensity distribution of the high-speed camera images taken in the tangential direction. We installed a plane mirror in the vacuum vessel and changed the camera lens to a wide-angle one (C-mount lens f = 16 mm) to expand the field of view, which was previously limited by the outer legs of TF coils. After the mirror installation we have become able to get the image in the whole region between inner and outer walls.

Under the condition of weak vertical field ($I_{PVF} <$ 350 A), the duration of the plasma current of tokamak discharge was improved by the external helical field. The outward plasma displacement was suppressed in tokamak discharge with the external helical field. The plasma was located stably in contact with the inner legs of the TF coils. These indicates that external helical field contributed to the horizontal position stability of the radial direction in the tokamak discharge under the condition of $I_{PVF} < 350$ A.

Acknowledgment

This work is performed with the support and under the auspices of the NIFS Collaboration Research program (NIFS14KOAP027) including the NIFS Joint Use Program of Measurement Instruments.

[1] H. Ikezi, K.F. Schwarzenegger and C. Ludescher, Phys. Fluids **22**, 2009 (1979).
[2] K. Sakurai and S. Tanahashi, J. Phys. Soc. Jpn. **49**, 759 (1980).
[3] W VII-A TEAM, Nucl. Fusion **20**, 1093 (1980).
[4] J. Fujita *et al.*, Plasma Physics and Controlled Nuclear Fusion Research (Proc. 8th Int. Conf., Brussels, Belgium, 1980) Vol.1, p.209.
[5] K. Yamazaki *et al.*, J. Plasma Fusion Res. SERIES **8**, 1044 (2009).
[6] R. Nishimura *et al.*, J. Plasma Fusion Res. **9**, 3402059 (2014).
[7] T. Sakito *et al.*, J. Plasma Fusion Res. **10**, 3402033 (2015).
[8] T. Oishi *et al.*, J. Plasma Fusion Res. SERIES **9**, 69 (2010).
[9] K. Yamazaki *et al.*, Fusion Technol. **21**, 147 (1992).